Underactuated Manipulator Robot Control via H_2, H_∞, H_2/H_∞, and μ-Synthesis Approaches: a Comparative Study

Adriano A. G. Siqueira
Member, ABCM
siqueira@sc.usp.br
University of São Paulo – USP
Engineering School of São Carlos
Mechanical Engineering Department
São Carlos, SP, Brazil

Marco H. Terra
terra@sc.usp.br
University of São Paulo – USP
Engineering School of São Carlos
Electrical Engineering Department
São Carlos, SP, Brazil

João Y. Ishihara
University of Brasília – UnB
Electrical Engineering Department
Brasília, DF, Brazil

Tácio L. S. Barbeiro
University of São Paulo – USP
Engineering School of São Carlos
Electrical Engineering Department
São Carlos, SP, Brazil

This paper deals with robust control of underactuated manipulator robots. It presents a comparative study of four combined controllers H_2, H_∞ , H_2/H_∞ and μ-synthesis, plus computed torque method. These controllers are applied in an actual underactuated manipulator robot with 3 degrees of freedom, of which joints can be configured as active or passive ones. The study performed in this paper compares the robustness of each controller when different disturbances are considered.
Keywords*: manipulator robot; computed torque method; robust control; μ synthesis; H_2, H_∞, H_2/H_∞*

Introduction

Mechanical manipulators have been used for the automation of repetitive tasks in industrial environments. These environments normally have easy physical access and low risk for the human health. However, in the last years, the use of manipulators in inhospitable environments of difficult access (such as in the interior of nuclear plants, the deep of the oceans and in the space) have increased. In this case, the occurrence of electrical or mechanical failures makes the maintenance of the manipulators more difficult and expensive. After the occurrence of a failure in the actuators, the manipulator can be considered an underactuated system.

This paper focuses on robust control of an underactuated manipulator robot of three joints and rigid links (see Bergeman (1996), Bergeman and Xu (1994), and references therein). Despite several controllers that appear in the literature, there is a lack of robust controllers applied to this kind of manipulator. The control of an underactuated robot is not trivial, due to uncertainties and disturbances present in manipulator robots, and, particularly, due to the difficulty in controlling free joints indirectly through active joints by dynamic coupling. The main objective of this work is to compare the robustness of four types of combined controllers when the underactuated system is subject to torque disturbances (combined controller means computed torque plus robust controller). Even for the control of totally actuated robot, Sage et al. (1999) states that the robustness of these combined controllers has not been tested in practice.

One of the most common techniques used in the control of manipulators is the partitioned controller or computed torque method Craig (1986), whose control law is divided in two parts. One of the parts is based on the nominal dynamic model of the plant and it is called *model based*, and basically transforms the multivariable nonlinear plant into a set of detached linear systems. The other part, called *error driven*, is responsible for the adjustment based on the error between the desired and real movements, i.e., the position and velocity errors. If there is perfect knowledge of all the robot's parameters and if the robot is not subject to external disturbances, the computed torque method is capable to provide excellent control quality. But model imperfections and external disturbances degrade the performance of this control system. To overcome this deficiency, this controller can be allied to a robust controller. The resulting control scheme consists of an inner loop feedback linearization controller, and an outer loop robust controller (see Control Methodologies and Design Procedure). Basic references for computed torque method can be seen in Craig (1986), and references therein, and more details of the robust controllers adopted in this work can be seen in Balas et al. (1994), Chiang and Safonov (1992), Craig (1986), Doyle et al. (1989), Doyle et al. (1992), Safonov et al. (1989), and also Zhou et al. (1994), Zhou et al. (1994a), Zhou et al. (1995), Zhou and Doyle (1998).

Robust control laws aim to keep the error and the output signals of the system under pre-specified tolerance levels, despite the effect of uncertainties. These uncertainties can be external (disturbances and noises) or internal (plant model imperfections) to the system. The robust control techniques adopted in this comparative study are based on H_2, H_∞, H_2/H_∞ and μ-synthesis approaches. The H_2 control technique is based on the minimization of the quadratic norm of the transfer function between the input disturbance signal and the plant's output signal. It is known that H_2 control does not present guaranteed robustness a priori, when unstructured uncertainties are present. This controller is considered here to be used as reference in the comparative analysis. The H_∞ control has the basic objective to minimize the effect of disturbances in the plant output, but, on the other hand, it presents limitations in the quality of the system's performance. The H_2/H_∞ mixed control joins the ability of the H_∞

Paper accepted June, 2009. Technical Editor: Fernando A. Forcellini

control to minimize the effect of input disturbances on the plant output with the performance of H_2 technique. In the μ-synthesis design, a perturbation matrix Δ is chosen and through an optimization sequence a stabilizing controller for the worst perturbation is obtained.

The main question addressed in this paper, with the comparison of four combined controllers for underactuated manipulators, is related with the structure of these controllers; despite the same γ parameter to be adjusted in the design of H_∞, H_2/H_∞ and μ controllers, the structures of these three controllers are different in nature (except when γ goes to the infinity; in this case, these robust controllers tend to the H_2 control, the robustness of H_∞, H_2/H_∞, and μ controllers increases when γ decreases). Let us suppose that after the robust controllers are designed, the respective γ's obtained are almost the same. Considering the performance of each controller, what are the differences among them before and after the disturbances are applied?

Underactuated Manipulator Robot

The system considered in this paper consists basically on a serial planar underactuated robot manipulator with 3 rigid links and fixed base. The joints and links are numbered from 1 to 3, with joint 1 and link 1 being the closest to the base. This underactuated arm showed in Fig.1, named UArm II, was designed and built by H. Ben Brown, Jr. of Pittsburgh, PA, USA. This 3-link manipulator has special-purpose joints containing each an actuator and a brake, so that they can act as active or passive joints. The manipulator configuration can be changed enabling or not the DC motor of each joint. For a general underactuated robot manipulator, it is used q to represent the robot's n×1 joint vector, and τ to represent its n×1 torque vector. For further details see Bergeman (1996).

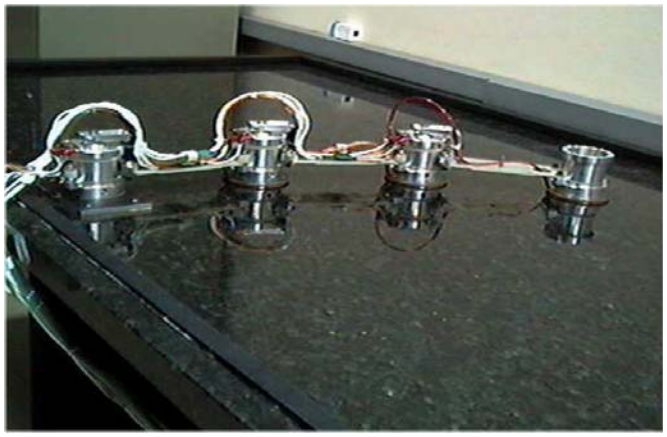

Figure 1. Underactuated manipulator, UArm II.

The dynamic equations of a manipulator are found in closed-form via the classical Lagrangian approach, as in Craig (1986), Lewis et al. (1993), and Bergeman and Xu (1994):

$$\tau = M(q)\ddot{q} + b(q,\dot{q}) \tag{1}$$

where $M(q) \in \Re^{n\times n}$ is the symmetric positive definite inertia matrix and $b(q, \dot{q}) \in \Re^{n\times 1}$ is the vector of Coriolis, centrifugal, gravitational, and frictional torques.

The dynamic equation of an underactuated manipulator can be obtained partitioning Eq. (1) into components, corresponding to the active and passive joints, as:

$$\begin{bmatrix}\tau_a\\ 0\end{bmatrix} = \begin{bmatrix}M_{aa}(q) & M_{au}(q)\\ M_{ua}(q) & M_{uu}(q)\end{bmatrix}\begin{bmatrix}\ddot{q}_a\\ \ddot{q}_u\end{bmatrix} + \begin{bmatrix}b_a(q,\dot{q})\\ b_u(q,\dot{q})\end{bmatrix} \tag{2}$$

where $b(q, \dot{q}) = C(q, \dot{q})+F(\dot{q})+G(q)$ and the subscripts a and u denote quantities related to the active and unlocked passive joints, respectively. It is considered that n_u joints of the manipulator are unactuated, and the remaining n_a joints operate normally. When $n_a > n_u$, one can define the following control strategy: in a first control phase, the n_u passive joints are driven to the set-points via their dynamic coupling with a subset of the active joints (n_u active joints are used to control and n_a–n_u active joints are kept locked), and are locked. In a second control phase, all the active joints are controlled.

For the first phase, factoring out $\ddot{q}_a$ in the second line of Eq. (2) and substituting it in the first one:

$$\tau_a = \overline{M}\ddot{q}_u + \overline{b} \tag{3}$$

where $\overline{M} = M_{au} - M_{aa}M_{ua}^{-1}M_{uu}$ and $\overline{b} = b_a - M_{aa}M_{ua}^{-1}b_u$.

Control Methodologies

This section contains the essential concepts of the computed torque, H_2, H_∞, H_2/H_∞ and μ-synthesis control theories. See Bernstein et al. (1989), Chiang and Safonov (1992), Craig (1986), Doyle et al. (1989), Safonov et al. (1989), and also Zhou et al. (1994), Zhou et al. (1994a), Zhou et al. (1995), Zhou and Doyle (1998) for further details.

Computed Torque Controller

The problem of controlling a nonlinear system like Eq. (1) can be handled by the computed torque method Craig (1986). The control law associated with this technique is given by:

$$\tau_a = \overline{M}_{est}(q)\tau_a' + \overline{b}_{est}(q,\dot{q}) \tag{4}$$

where $\overline{M}_{est}(q)$ is an estimated model of the underactuated robot's inertial parameter, $\overline{M}(q)$. Likewise, $\overline{b}_{est}(q,\dot{q})$ is an estimated model of the vector of non-inertial elements $\overline{b}(q,\dot{q})$.

The vector τ_a' is computed as follows:

$$\tau_a' = \ddot{q}_u^d + K_v\left(\dot{q}_u^d - \dot{q}_u\right) + K_p\left(q_u^d - q_u\right) \tag{5}$$

where $\left\{q_u^d, \dot{q}_u^d, \ddot{q}_u^d\right\}$ represent the desired trajectory, desired velocity and desired acceleration of the controlled joints, and K_p and K_v are n×n diagonal matrices with positive scalar elements. The closed-loop equation for the whole system is derived from Eqs. (4) and (5):

$$\ddot{e} + K_v\dot{e} + K_p e = \overline{M}_{est}^{-1}(q)\left[\left(\overline{M}(q) - \overline{M}_{est}(q)\right)\ddot{q} + \overline{b}(q,\dot{q}) - \overline{b}_{est}(q,\dot{q})\right] \tag{6}$$

where $e = q_u^d - q_u$.

In a real case, there exist disturbances that are not modelled properly, such as joint friction, torque variation on the actuators, and perturbations due to possible loads carried by the manipulator.

Defining these disturbances as $\bar{d}_{ext}(q,\dot{q})$ and adding them to Eq. (6), one has:

$$\ddot{e}+K_v\dot{e}+K_p e=\bar{M}_{est}^{-1}\left[(\bar{M}-\bar{M}_{est})\ddot{q}+\bar{b}(q,\dot{q})-\right.$$
$$\left.-\bar{b}_{est}(q,\dot{q})+\bar{d}_{ext}(q,\dot{q})\right]. \quad (7)$$

If all the robot's parameters are known with absolute precision $\bar{M}(q)=\bar{M}_{est}(q)$ and $\bar{b}_{est}(q,\dot{q})=\bar{d}_{ext}(q,\dot{q})$, and in the absence of disturbances $(\bar{d}_{ext}(q,\dot{q})=0)$, the right size of Eq. (7) is zero, and the computed torque method is able to provide excellent quality of control. The dynamic equation for this ideal system, driven by a control signal $u(t)$ is:

$$\begin{bmatrix}\dot{e}\\ \ddot{e}\end{bmatrix}=\begin{bmatrix}0 & I\\ -K_p & -K_v\end{bmatrix}\begin{bmatrix}e\\ \dot{e}\end{bmatrix}+\begin{bmatrix}0\\ I\end{bmatrix}u\,. \quad (8)$$

H_2, H_∞ and H_2/H_∞ Controllers

The control systems presented in this section are described by the block diagram displayed in Fig. 2. This diagram contains two main blocks, the plant $P(s)$ and the controller $K(s)$ (the operator s will be omitted in the equations). The plant has two sets of input signals, the internal input u and the external input w, and two sets of output signals, the measured signal y and the regulated output z. The transfer function matrix $P(s)$ and its realization are given by Zhou et al. (1995):

$$\begin{bmatrix}P_{11} & P_{12}\\ P_{21} & P_{22}\end{bmatrix}=\left[\begin{array}{c|cc}A & B_1 & B_2\\ \hline C_1 & D_{11} & D_{12}\\ C_2 & D_{21} & 0\end{array}\right]=\left[\begin{array}{c|c}A & B\\ \hline C & D\end{array}\right] \quad (9)$$

and

$$z=P_{11}w+P_{12}u \qquad y=P_{21}w+P_{22}u \qquad u=Ky \quad (10)$$

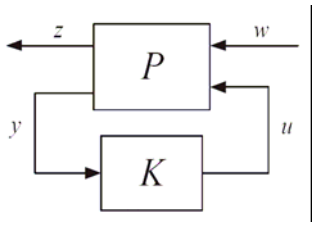

Figure 2. Block diagram for the H_2, H_∞ and H_2/H_∞ control systems.

Combining the equations in Eq. (10), one obtains the closed loop transfer function $T_{zw}(s)$ between the external inputs w and regulated outputs z, which is given in terms of linear fractional transformation (LFT):

$$T_{wz}(s)=F_l(P,K)=P_{11}+P_{12}K(I-P_{22}K)^{-1}P_{21}\,.$$

1) H_2 Control: The H_2 control approach aims to find a real, rational and proper controller $K(s)$, which internally stabilizes $P(s)$ and minimizes the H_2 norm of the transfer matrix $T_{zw}(s)$. The solution of the H_2 control problem involves the resolution of two Algebraic Riccati Equations (ARE's) associated to the Hamiltonian matrices given by H_2 and J_2:

$$H_2=\begin{bmatrix}A-B_2D_{12}^TC_1 & -B_2B_2^T\\ -C_1^TC_1+C_1^TD_{12}D_{12}^TC_1 & -A^TC_1^TB_2^T\end{bmatrix}$$
$$J_2=\begin{bmatrix}A^T-C_2^TD_{12}B_1^T & -C_2^TC_2\\ -B_1B_1^T+B_1D_{21}^TD_{21}B_1^T & -A+B_1D_{21}^TC_2\end{bmatrix}$$

Defining:

$$F_2:=-\left(B_2^TX_2+D_{12}^TC_1\right)\quad L_2:=-\left(Y_2C_2^T+B_1D_{21}^T\right)\quad \hat{A}_2:=A+B_2F_2+L_2C_2$$

where $X_2 = Ric(H_2)$ and $Y_2 = Ric(J_2)$, there exists an optimal and unique H_2 controller given by Zhou et al. (1995):

$$K_{opt}(s):=\left[\begin{array}{c|c}\hat{A}_2-B_2D_KC_2 & -\left(L_2-B_2D_K\right)\\ \hline F_2-D_KC_2 & D_K\end{array}\right]$$

with $D_K:=-D_{12}^TD_{11}D_{21}^T$.

2) H_∞ Control: The H_∞ control approach aims to find a real, rational and proper controller $K(s)$, which internally stabilizes $P(s)$ and minimizes the H_∞ norm of the transfer matrix $T_{zw}(s)$, which is defined as:

$$\left\|T_{z\omega}\right\|_\infty=\sup_{\omega\in\Re}\bar{\sigma}\{T_{z\omega}(j\omega)\} \quad (11)$$

where $\sup\bar{\sigma}\{.\}$ denotes the supremum of the maximum singular value. The H_∞ solution involves the resolution of two ARE's associated to the Hamiltonian matrices given by H_∞ and J_∞, and can be seen in details in Zhou et al. (1995):

$$H_2:=\begin{bmatrix}A-B_2D_{12}^TC_1 & -B_2B_2^T\\ -C_1^TC_1+C_1^TD_{12}D_{12}^TC_1 & -A^TC_1^TB_2^T\end{bmatrix}$$
$$J_2:=\begin{bmatrix}A^T-C_2^TD_{12}B_1^T & -C_2^TC_2\\ -B_1B_1^T+B_1D_{21}^TD_{21}B_1^T & -A+B_1D_{21}^TC_2\end{bmatrix}$$

where

$$R:=D_{1\bullet}^TD_{1\bullet}-\begin{bmatrix}\gamma^2I & 0\\ 0 & 0\end{bmatrix}$$
$$\tilde{R}:=D_{\bullet1}D_{\bullet1}^T-\begin{bmatrix}\gamma^2I & 0\\ 0 & 0\end{bmatrix}$$
$$D_{1\bullet}:=\begin{bmatrix}D_{11} & D_{12}\end{bmatrix}$$
$$D_{\bullet1}:=\begin{bmatrix}D_{11}\\ D_{21}\end{bmatrix}$$

and the Riccati equation solutions related to the Hamiltonians are denoted by

$$X_\infty:=Ric(H_\infty),\quad Y_\infty:=Ric(J_\infty).$$

The feedback and output injection gains are given by

$$F_\infty:=\begin{bmatrix}F_{1\infty}\\ F_{2\infty}\end{bmatrix}:=-R^{-1}\left[D_{1\bullet}^TC_1+B^TX_\infty\right]$$
$$L_\infty:=\begin{bmatrix}L_{1\infty} & L_{2\infty}\end{bmatrix}=\left[B_1D_{\bullet1}^T+Y_\infty C^T\right]\tilde{R}^{-1}$$

and can be partitioned with D as follows:

$$\left[\begin{array}{c|c} & F_\infty^T \\ \hline L_\infty^T & D \end{array}\right] = \left[\begin{array}{c|ccc} & F_{11\infty}^T & F_{12\infty}^T & F_{2\infty}^T \\ \hline L_{11\infty}^T & D_{1111} & D_{1112} & 0 \\ L_{12\infty}^T & D_{1121} & D_{1122} & I \\ L_{2\infty}^T & 0 & I & 0 \end{array}\right]$$

All the rational internally stabilizing controllers $K(s)$ such that $\|T_{z\omega}(s)\|_\infty \le \gamma$ are given by $K = F_l(M_\infty, Q)$ for arbitrary $Q \in RH_\infty$ such that $\|Q\| < \gamma$, where

$$M_\infty = \left[\begin{array}{c|cc} \hat{A} & \hat{B}_1 & \hat{B}_2 \\ \hline \hat{C}_1 & \hat{D}_{11} & \hat{D}_{12} \\ \hat{C}_2 & \hat{D}_{21} & 0 \end{array}\right] \tag{12}$$

$$\hat{D}_{11} = -D_{1121}D_{1111}^T\left(\gamma^2 I - D_{1111}D_{1111}^T\right)^{-1}D_{1112} - D_{1122}$$

$\hat{D}_{12}$ and $\hat{D}_{21}$ are any matrices (Cholesky factors) satisfying:

$$\hat{D}_{12}\hat{D}_{12}^T = I - D_{1121}\left(\gamma^2 I - D_{1111}^T D_{1111}\right)^{-1}D_{1121}^T$$
$$\hat{D}_{21}^T\hat{D}_{21} = I - D_{1121}\left(\gamma^2 I - D_{1111}D_{1111}^T\right)^{-1}D_{1112}^T$$

and

$$\hat{B}_2 = Z_\infty\left(B_2 + L_{12\infty}\right)\hat{D}_{12}$$
$$\hat{C}_2 = -\hat{D}_{21}\left(C_2 + F_{12\infty}\right)$$
$$\hat{B}_1 = -Z_\infty L_{2\infty} + \hat{B}_2\hat{D}_{12}^{-1}\hat{D}_{11}$$
$$\hat{C}_1 = F_{2\infty} + \hat{D}_{11}\hat{D}_{21}^{-1}\hat{C}_2$$
$$\hat{A} = A + BF_\infty + \hat{B}_1\hat{D}_{21}^{-1}\hat{C}_2$$
$$Z_\infty = \left(I - \gamma^{-2}Y_\infty X_\infty\right)^{-1}$$

where $\gamma > max\left(\bar{\sigma}\left[D_{1111}^T D_{1112}^T\right], \bar{\sigma}\left[D_{1111}D_{1112}\right]\right)$ and $\rho(X_\infty Y_\infty) < \gamma^2$.

3) Mixed H_2 /H_∞ Control: The mixed H_2 /H_∞ control aims to provide to the closed loop system H_2 performance with H_∞ constraint for attenuation of input disturbances, which can be formulated as follows: given the system P of Eq. (9) stabilizable and detectable, find a controller of same dimension of P

$$\dot{x}_k = A_k x_k + B_k y \tag{13}$$

$$u = c_k x_k \tag{14}$$

that satisfies the following design criteria:

(i) the closed loop system is asymptotically stable;

(ii) the transfer function T_{zw} satisfies the constraint $\|T_{z\omega}\|_\infty \le \gamma$, with $\gamma > 0$;

(iii) the expression

$$J\left(A_k, B_k, C_k\right) = \lim_{t\to\infty}\frac{1}{t}\int_0^T\left[x(\upsilon)^T R_1 x(\upsilon) + u(\upsilon)^T R_2 u(\upsilon)\right]d\upsilon$$

is minimized, where $R_1 = E_1^T E_1 \ge 0$, $R_2 = E_2^T E_2 \ge 0$ and $E_1^T E_2 = 0$.

The (A_k,B_k,C_k) controller presented in Bernstein and Haddad (1989) that satisfies these design criteria is given by:

$$A_k = A - X_{2/\infty}\Gamma - \sum Y_{2/\infty}S + \gamma^{-2}X_{2/\infty}R_{1\infty}$$
$$B_k = X_{2/\infty}C_2^T V^{-1}$$
$$C_k = -R_2^{-1}B_2^T Y_{2/\infty}S$$

where

$$S = \left(I_n + \beta^2\gamma^{-2}Z_{2/\infty}Y_{2/\infty}\right)^{-1}$$
$$\Gamma = C_2^T V^{-1}C_2$$
$$\sum = B_2 R_2^{-1}B_2^T$$
$$V = D_{12}D_{12}^T$$

and

$$AX_{2/\infty} + X_{2/\infty}A^T + B_1B_1^T + \gamma^{-2}X_{2/\infty}R_{1\infty}X_{2/\infty} - X_{2/\infty}\Gamma X_{2/\infty} = 0 \tag{15}$$

$$\left[A + \gamma^{-2}\left(X_{2/\infty} + Z_{2/\infty}\right)R_{1\infty}\right]^T Y_{2/\infty} + Y_{2/\infty}\left[A + \gamma^{-2}\left(X_{2/\infty} + Z_{2/\infty}\right)R_{1\infty}\right] + \\ + R_1 - S'Y_{2/\infty}\sum Y_{2/\infty}S = 0 \tag{16}$$

$$\left(A - \sum Y_{2/\infty}S + \gamma^{-2}X_{2/\infty}R_{1\infty}\right)Z_{2/\infty} + Z_{2/\infty}\left(A - \sum Y_{2/\infty}S + \gamma^{-2}X_{2/\infty}R_{1\infty}\right)^T + \\ + \gamma^{-2}Z_{2/\infty}\left(R_{1\infty} + \beta^2 S^T Y_{2/\infty}S\right)Z_{2/\infty} + X_{2/\infty}\Gamma X_{2/\infty} = 0 \tag{17}$$

where $X_{2/\infty}$, $Y_{2/\infty}$, $Z_{2/\infty}$ are semi-definite positive matrices. It is adopted here $R_{1\infty} = R1$, the root square of this matrix defines the output matrix of the transfer function to be minimized in the H_∞ criterion. Further details can be seen in Bernstein and Haddad (1989), Zhou et al. (1994), and Zhou et al. (1994a).

μ-Synthesis

μ-Synthesis aims to solve the following optimization problem:

$$\min_K \inf_{D, D^{-1}\in H_\infty}\left\|DF_l(P,K)D^{-1}\right\|_\infty \tag{18}$$

where $K(s)$ and $D(s)$ are found iteratively. This procedure is called *D-K iteration* that can be summarized in the following steps:

1) Fix an initial estimate of the scaling matrix $D_\omega \in \mathbf{D}$ pointwise across frequency;
2) Find scalar transfer functions $d_i(s)$, $d_i^{-1}(s) \in RH_\infty$ for $i = 1, 2, ..., (F-1)$ such that $|d_i(j\omega)| \approx d_i^\omega$. This step can be done using the interpolation theory Youla and Saito (1967);
3) Let $D(s) = \text{diag}(d_1(s)I, ..., d_{F-1}(s)I, I)$. Construct a state space model for the system:

$$\hat{P}(s) = \left[\begin{array}{cc} D(s) & \\ & I \end{array}\right]P(s)\left[\begin{array}{cc} D^{-1}(s) & \\ & I \end{array}\right].$$

4) Solve an H_∞ – optimization problem to minimize:

$$\left\|F_l\left(\hat{P}, K\right)\right\|_\infty \le \gamma \tag{19}$$

over all stabilizing K's. Note that this optimization problem uses the scaled version of $P(s)$. Let its minimizing controller be denoted by $\hat{K}(s)$;

5) Minimize $\bar{\sigma}\left[D_\omega F_l\left(P, \hat{K}\right)D_\omega^{-1}\right]$ over D_ω, pointwise across frequency. Note that this evaluation uses the minimizing $\hat{K}(s)$ from the last step, but that $P(s)$ is unscaled. The

minimization itself produces a new scaling function. Let this new function be denoted by $\hat{D}_\omega$;

6) Compare $\hat{D}_\omega$ with the previous estimate D_ω. Stop if they are close, otherwise replace D_ω with $\hat{D}_\omega$ and return to step (2).

Details of how this controller can be designed are presented in Balas et al. (1994), and Zhou et al. (1995).

Combined Controller

It is well known that modelling imperfections and external disturbances degrade the computed torque control performance Kang et al. (1999). To overcome this problem, the computed torque technique can be improved

The combined controller, Fig. 3, basically has the same structure of a robust controller for a linear system. The weighting function $W_e(s)$ is used to shape the system performance on the frequency domain, and $W_\Delta(s)$ shapes the multiplicative unstructured uncertainties in the input of the plant, representing possible errors in the manipulator's actuators, unmodelled high frequency dynamics, or uncertain zeros on the right half plane, Zhou and Doyle (1998).

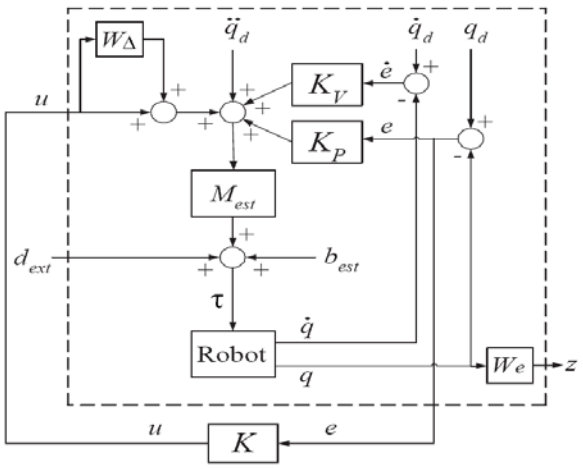

Figure 3. Block diagram of the complete control structure scheme.

The portion of Fig. 3 delimited by the dotted line (computed torque, parametric uncertainties representation, weighted performance) is the augmented plant $P(s)$, used to calculate the linear H_2, H_∞, H_2/H_∞ and μ controllers. The controller designs consist of two steps. In the first step the computed torque method is used to pre-compensate the dynamics of the nominal plant. In the second step the controllers H_2, H_∞, H_2/H_∞ and μ are used to post-compensate the residual error which is not completely removed by the computed torque method. Thus, the combined controller is able to perform robust tracking control (we include the H_2 control in this category to facilitate our presentation, though it is known the robustness limitations of this controller).

Design Procedure

The MATLAB *Robust* toolbox was utilized to design the H_2, H_∞, and μ controllers. The H_2/H_∞ is computed following the algorithm given in Section Control Methodologies. To synthesize the controllers, the first step is to find the state space realization of the augmented plant $P(s)$. Thus, the K_p, K_v, $W_e(s)$ and $W_\Delta(s)$ values must be defined. Given K_p and K_v of the computed torque method, it is obtained the linearized system given by Eq. (8). The following state equations define this system:

$$\dot{x} = A_g x + B_g u \tag{20}$$

$$y = C_g x + D_g u \tag{21}$$

The vector $x \in \Re^m$ represents the states of the plant, and it is defined as:

$$x = \begin{bmatrix} e \\ \dot{e} \end{bmatrix} = \begin{bmatrix} q^d - q \\ \dot{q}^d - \dot{q} \end{bmatrix} \tag{22}$$

and the matrices $A_g \in \Re^{m\times m}$, $B_g \in \Re^{m\times n}$, $C_g \in \Re^{n\times m}$ and $D_g \in \Re^{n\times n}$ as:

$$A = \begin{bmatrix} 0 & I \\ -K_p & -K_v \end{bmatrix} \quad B_g = \begin{bmatrix} 0 \\ I \end{bmatrix} \quad C_g = \begin{bmatrix} I & 0 \end{bmatrix} \tag{23}$$

and $D_g = 0$. For a manipulator with three joints totally actuated, $n = 3$ and $m = 6$, with only two actuated joints, $n = 2$ and $m = 4$, and with one actuated joint, $n = 1$ and $m = 2$. The K_p and K_v gains are $n\times n$ diagonal matrices adjusted iteratively following an heuristic criterion.

The performance objectives $W_e(s)$ and $W_\Delta(s)$ are related to the frequency response of the sensitivity function $S(s) = (I + P(s)K(s))^{-1}$. Defining the natural frequency ω_n, the damping ratio ε, the bandwidth ω_b and the peak sensitivity Ms, the following performance weighting function can be determined:

$$W_e(s) = diag\{F_{e,1}(s),...,F_{e,n}(s)\}\, F_{e,i}(s) = \frac{\frac{s}{M_s} + \omega_b}{s + \omega_b \varepsilon}$$

where $i = 1, ..., n$. Choosing the maximum gain M_u of $K(s)S(s)$ (controller and sensibility function), the controller bandwidth ω_{bc} and a small $\varepsilon_1 > 0$, the following control weighting function $W_\Delta(s)$ can be selected:

$$W_\Delta(s) = diag\{F_{\Delta,1}(s),...,F_{\Delta,n}(s)\}\, F_{\Delta,i}(s) = \frac{s + \frac{\omega_{bc}}{M_u}}{\varepsilon_1 s + \omega_{bc}} .$$

The weighting functions $W_e(s)$ and $W_\Delta(s)$ are selected such that

$$\left|W_e(j\omega)\right|^{-1} \geq \left|S(j\omega)\right| \tag{24}$$

$$\left|W_\Delta(j\omega)\right|^{-1} \geq \left|K(j\omega)S(j\omega)\right| \;; \quad \forall \omega. \tag{25}$$

The state space matrices of the augmented system are given by:

$$A = \begin{bmatrix} 0 & I & 0 & 0 \\ -K_p & -K_v & 0 & 0 \\ 0 & 0 & Aw_\Delta & 0 \\ B_{W_e} & 0 & 0 & A_{W_e} \end{bmatrix} \quad B_1 = \begin{bmatrix} 0 & 0 \\ I & 0 \\ 0 & 0 \\ 0 & B_{W_e} \end{bmatrix}$$

$$B_2 = \begin{bmatrix} 0 \\ I \\ B_{W_\Delta} \\ 0 \end{bmatrix} \qquad C_1 = \begin{bmatrix} 0 & 0 & C_{W_\Delta} & 0 \\ D_{W_e} & 0 & 0 & 0C_{W_e} \end{bmatrix}$$

$$C_2 = \begin{bmatrix} I & 0 & 0 & 0 \end{bmatrix} \quad D_{11} = \begin{bmatrix} 0 & 0 \\ 0 & D_{W_e} \end{bmatrix} \quad D_{12} = \begin{bmatrix} D_{W_\Delta} \\ 0 \end{bmatrix}$$

$$D_{21} = \begin{bmatrix} 0 & I \end{bmatrix} \quad \text{and} \quad D_{22} = \begin{bmatrix} 0 \end{bmatrix}$$

where ($A_{W\Delta}$, $B_{W\Delta}$, $C_{W\Delta}$, $D_{W\Delta}$) is the state space realization for the weighting function $W_\Delta(s)$, and (A_{We} , B_{We} , C_{We} , D_{We}) for $W_e(s)$.

Finally, the state space realization of the augmented plant, $P(s)$, used for the design of the H_2 , H_∞, and μ controllers, is:

$$P = \left[\begin{array}{cccc|ccc} 0 & I & 0 & 0 & 0 & 0 & 0 \\ -K_p & -K_v & 0 & 0 & I & 0 & I \\ 0 & 0 & A_{W_\Delta} & 0 & 0 & 0 & B_{W_\Delta} \\ B_{W_e} & 0 & 0 & A_{W_e} & 0 & B_{W_e} & 0 \\ \hline 0 & 0 & C_{W_\Delta} & 0 & 0 & 0 & D_{W_\Delta} \\ D_{W_e} & 0 & 0 & C_{W_e} & 0 & D_{W_e} & 0 \\ I & 0 & 0 & 0 & 0 & I & 0 \end{array}\right].$$

Experimental Results

All combined robust control techniques presented in Section Control Methodologies were implemented in the experimental underactuated manipulator UArm II, see Fig.1. To check the robustness of these combined controllers, torque disturbance tests were implemented considering the APA configuration, i.e., the first and third joints are actives and the second is passive. For this configuration, two control phases are necessary to control all joints to the set-point. In the first phase, the passive joint $q_u = q_2$ is controlled by the active joint 1, i.e., $q_a = q_1$ in 3. The joint 3 is kept locked in this phase. In the second phase, the active joints are controlled and $q_a = [q_1\ q_3]^T$. The passive joint 2 is kept locked, since it has already reached the set-point.

The tests are performed adding external torque disturbances in the first joint, during the first control phase, at different times

$$\tau_{d_1} = 0.5e^{-3(t-d_1)} \sin\left(4\pi\left(t - t_{d_1}\right)\right) \tag{26}$$

where $t_{d1} = 0.25s$, and

$$\tau_{d_2} = 0.3e^{\frac{-(t-d_2)^2}{2\mu^2}} \sin\left(0.8\pi\left(t - t_{d_2}\right)\right) \tag{27}$$

where $\mu = 0.3$ and $t_{d2} = 1.0\ s$. In order to establish common criteria to compare these combined controllers (the robust controllers were deduced taking into account different control problems; H_2 , H_∞ mixed H_2/H_∞, and μ-synthesis, plus a PD controller), two measurements are used: total applied torque and total position error, see Logan (1994), and Yao and Tomizuka (1994). These measurements are defined as follows:

$$E_\tau = \int_0^{T_f} \left|\tau(t)\right| dt, \qquad \mathsf{L}_2 = \left(\frac{1}{T_f}\int_0^{T_f} \left\|e\right\|_2^2 dt\right)^{\frac{1}{2}}. \tag{28}$$

Table 1. Robot parameters.

Link	m_i (kg)	I_i (kgm^2)	l_i (m)	l_{ci} (m)
1	0.850	0.0075	0.203	0.096
2	0.850	0.0075	0.203	0.096
3	0.625	0.0060	0.203	0.077

Table 2. K_p and K_v values for all controllers.

Configuration	K_p	K_v
APA, phase 1	$\begin{bmatrix} 20 \end{bmatrix}$	$\begin{bmatrix} 20 \end{bmatrix}$
APA, phase 2	$\begin{bmatrix} 10 & 0 \\ 0 & 20 \end{bmatrix}$	$\begin{bmatrix} 5 & 0 \\ 0 & 20 \end{bmatrix}$

Table 3. M_s, ω_b and ε values for all controllers.

Configuration	M_s	ω_b (rad/s)	ε (%)
APA, phase 1	1.1	1	0.01
APA, phase 2	1.5	1	0.01

Table 4. M_u, ω_{bc} and ε_1 values for all controllers.

Configuration	M_u	ω_{bc} (rad/s)	ε_1
APA, phase 1	20	10^6	1
APA, phase 2	50	10^6	1

The parameters utilized to determine $M(q)$ and $b(q,\dot{q})$ of Eq. (1) are displayed in Table 1. For all combined controllers are used the same K_p and K_υ (see Table 2). They were chosen heuristically in the middle of the interval, where these gains are adjusted to guarantee the stability of the real system. The weighting functions $W_e(s)$ and $W_\Delta(s)$ were defined using the parameters of Tables 3 and 4, respectively. The parameters to the H_2/H_∞ controller design were defined as

$$E_1 = \begin{bmatrix} 1 & 0 & 0 & -1 \\ 0 & 0 & 0 & 0 \end{bmatrix} \qquad E_2 = \begin{bmatrix} 0 & 0.01 \end{bmatrix}^T$$

for the first control phase, and

$$E_1 = \begin{bmatrix} 1 & 0 & 0 & 0 & -1000 & - & -1 & 0 \\ 0 & 1 & 0 & 0 & 0 & -1000 & 0 & -1 \\ 0 & 0 & 0 & 0 & 0 & 0 & 0 & 0 \end{bmatrix}$$

$$E_2 = \begin{bmatrix} 0 & 0 & 10 \end{bmatrix}^T$$

for the second control phase and $\beta = 0.1$ for both control phases. It is defined also, to the H_2/H_∞ controller design, $C_2 = E_1$, this choice was motivated by the necessity of the controller to satisfy the performance criteria defined in Eq.(24) and Eq.(25); and also to satisfy numerical convergence requirements. The γ values obtained from the robust controllers are shown in Table 5.

Table 5. H_∞, H_2/H_∞ and μ controllers.

Configuration	H_∞	H_2/H_∞	μ iteration 1	μ iteration 2
APA, phase 1	1.43	1.05	1.43	0.99
APA, phase 2	0.94	0.999	0.94	0.92

For all experiments, the initial position and the desired final position were $q(0) = [0^o\ 0^o\ 0^o]^T$ and $q(T_1,T_2) = [30^o\ 20^o\ 10^o]^T$, respectively, where $T_1 = [0.5]s$ and $T_2 = [2.0\ 4.0]s$ are respectively the desired trajectory times for the control phases 1 (when only the joint 2 is controlled) and 2 (when the joints 1 and 3 are controlled). Note that for the first control phase there is no trajectory reference for the joints 1 and 3 (the joint 3 is locked in this phase). The joint positions and torques for all controllers are shown in Figs. 4 to 7.

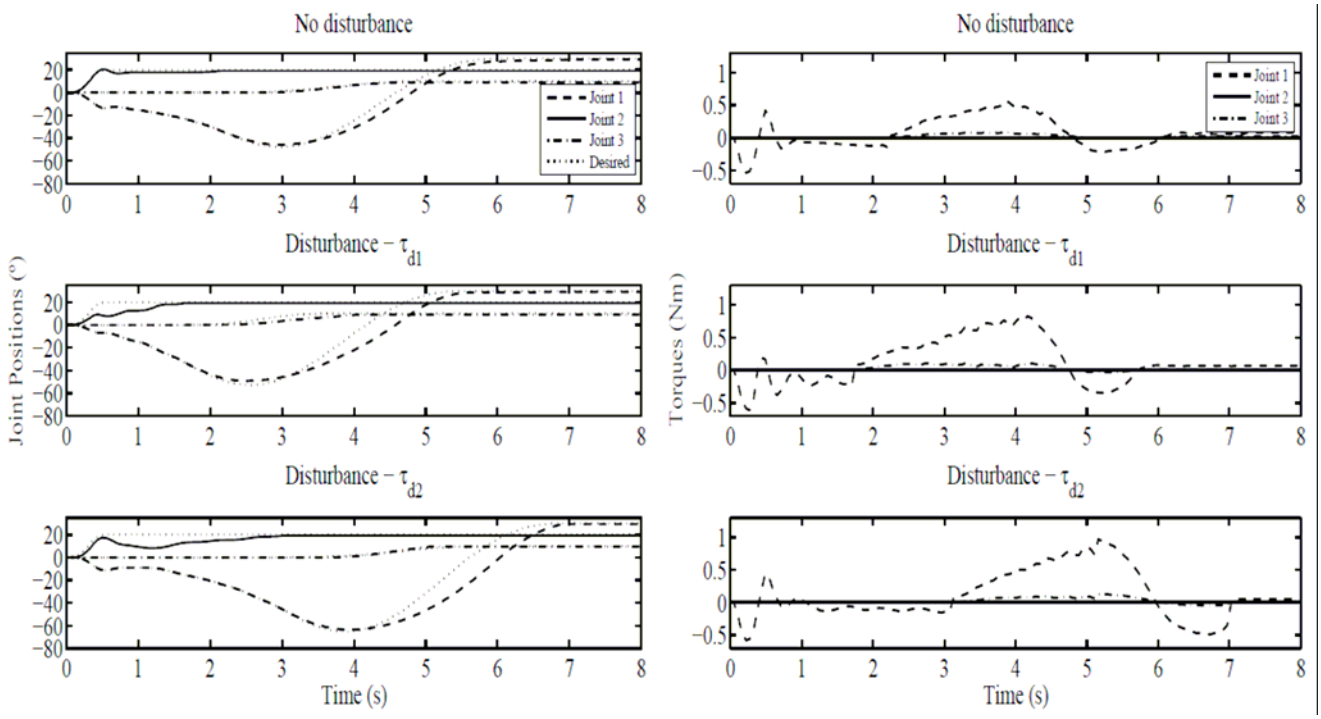

Figure 4. Joint positions and torques, H_2 controller.

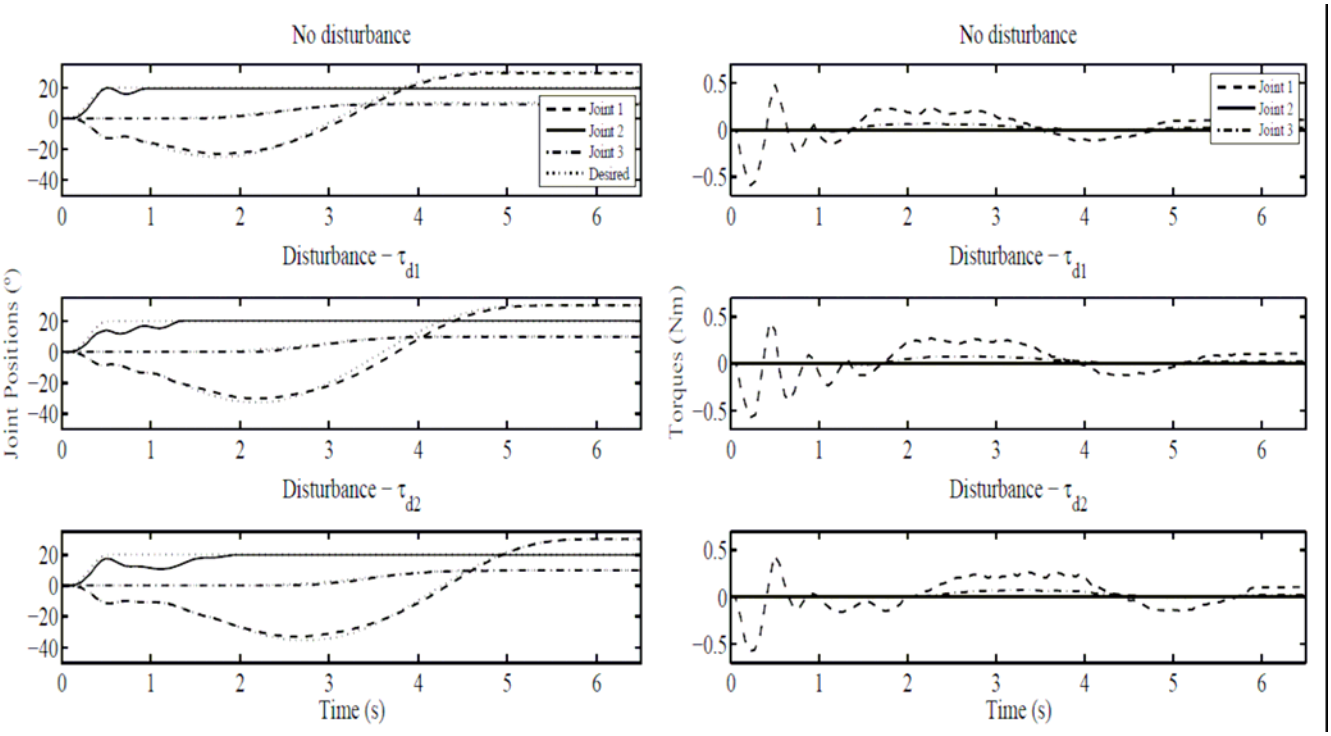

Figure 5. Joint positions and torques, H_∞ controller.

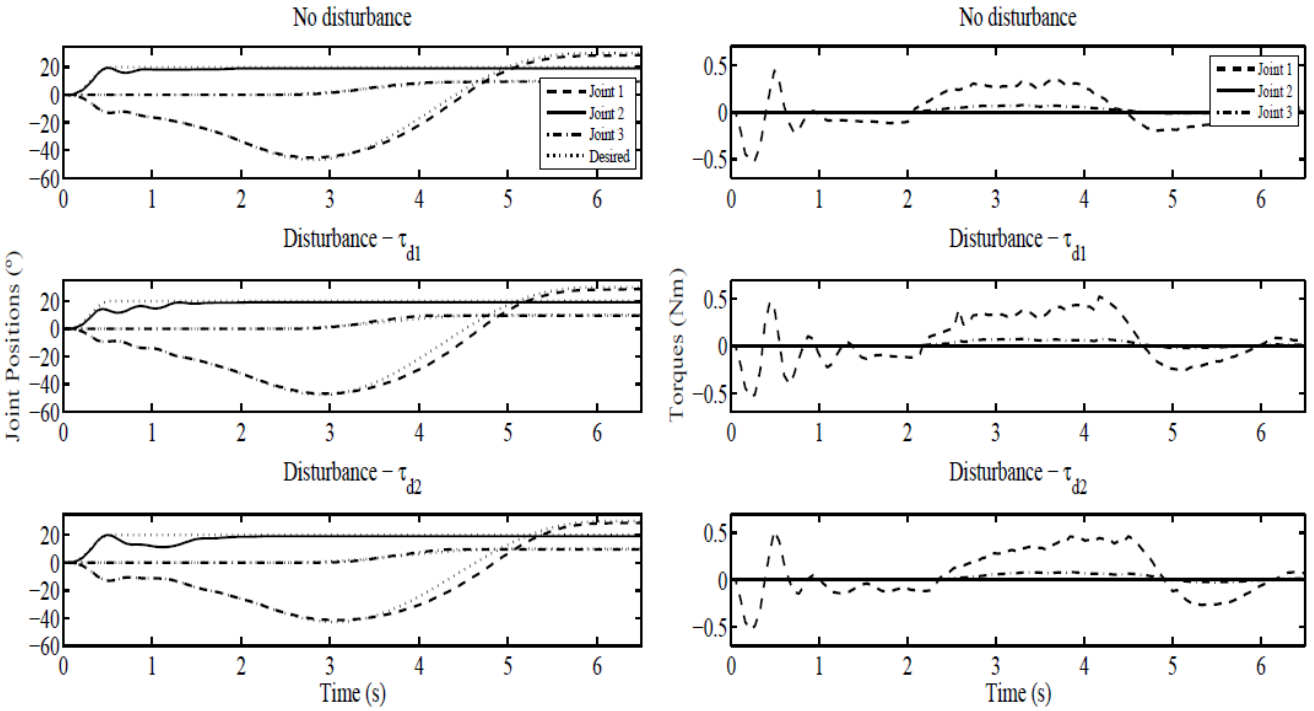

Figure 6. Joint positions and torques, H_2/H_∞ controller.

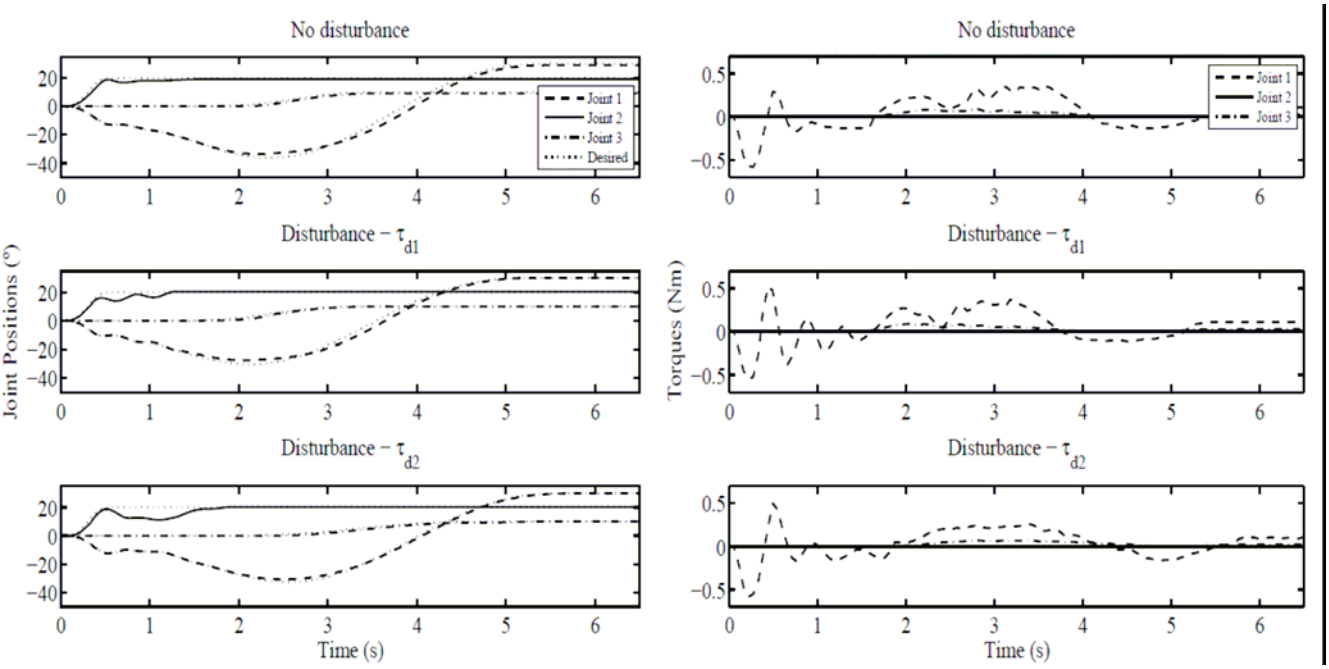

Figure 7. Joint positions and torques, μ controller.

In order to compare these controllers it is adopted two analysis references: H_2 controller and γ parameter.

H_2 as Reference

It is considered first the H_2 controller as reference. This choice is motivated by the fact that when γ goes to the infinity, the robust controllers tend to H_2 control. The robustness of H_∞ , H_2/H_∞ and μ controllers increases when γ decreases. Table 6, with the results without external disturbances, shows that the smallest total torque $E_t(.)$, see Eq. (28), is given by the H_∞ controller; the smallest position error $L_2(.)$ is given by the H_2/H_∞ controller (this index effectively determines the robustness of these controllers). Only the model uncertainties define the

differences between the robust controllers and the H_2 controller. One can observe that there exists some equivalence among the position error indexes $L_2(.)$ of the robust controllers and that the performance indexes of the H_2 controller are bigger than the values of the robust controllers.

In presence of external disturbances, the μ controller presents the best robustness, as it was expected, see Tables 7 and 8, the smallest $L_2(.)$ is given by the μ synthesis. Also from Tables 7 and 8, the smallest $E_\tau(.)$ is given by the H_∞ controller. For these cases, the performance indexes of the H_2 controller are two times bigger than the values of the robust controllers.

Table 6. Performance Indexes – without disturbance.

Configuration	E_τ (Nms)	L_2 ([°]^2)
H_2	1.78	4.9
H_∞	1.09	3.6
H_2/H_∞	1.41	3.1
μ-synthesis	1.31	3.8

Table 7. Performance Indexes – disturbance τ_{d1}, Eq. (26).

Configuration	E_τ (Nms)	L_2 ([°]^2)
H_2	2.54	12.6
H_∞	1.13	6.8
H_2/H_∞	1.70	6.1
μ-synthesis	1.20	4.6

Table 8. Performance Indexes – disturbance τ_{d2}, Eq. (27).

Configuration	E_τ (Nms)	L_2 ([°]^2)
H_2	2.76	14.9
H_∞	1.34	7.7
H_2/H_∞	1.80	7.2
μ-synthesis	1.36	6.7

γ Parameter as Reference

The second comparison performed takes into account the γ parameter as reference. This parameter indicates the disturbance rejection level of the robust controllers. It is compared firstly the γ effect for the controllers H_2/H_∞ and μ with the data of Table 5. They are close for both control phases: 1.05 and 0.99, for the first control phase; 0.999 and 0.92, for the second control phase, respectively. However, one can observe from Tables 6, 7, and 8, that position errors $L_2(.)$ for these controllers are not equivalent. Hence, the values of γ do not indicate properly the differences between the robustness of both controllers.

Even in comparison with H_∞ controller, the γ parameter does not display exactly how much the μ controller is more robust (despite the apparent proximity of both structures, μ is derived from the H_∞ controller via D scaling). The H_∞ controller is minimized for both control phases with $\gamma_{opt} = 1.43$ and $\gamma_{opt} = 0.94$, respectively. One can observe, mainly for the first disturbance, the differences between the disturbance rejections, for the μ controller and for the H_∞ controller. γ indicates how much each controller is robust, but it does not indicate how much one controller is more robust than other one.

Conclusions

In this paper, three robust controllers based on computed torque and H_∞, H_2/H_∞ and μ-synthesis techniques were implemented in an actual underactuated robot manipulator. These controllers are compared with the non-robust H_2 controller. The results presented in section "Experimental Results" along with the computed performance indexes show the differences of robustness among these combined controllers. From the results, the best performance, as it was expected, was presented by the μ-synthesis approach. However, a disadvantage of the μ-synthesis controller is the extra computational effort necessary to design it.

References

Balas, G.J., Doyle, J.C., Glover, K., Packard, A., Smith, R., 1994, "μ-Analysis and Synthesis Toolbox", The MathWorks.

Beaven, R.W., Wright, M.T., Seaward, D.R., 1996, "Weighting function selection in the H_∞ design process", *Control Engineering Practice*, Vol. 4, pp. 625-633.

Bernstein, D.S., Haddad, W.M., 1989, "LQG control with an H_∞ performance boud: a Riccati equation approach", *IEEE Transactions on Automatic Control*, Vol. 34, pp. 293-305.

Bergerman, M., 1996, "Dynamics and control of underactuated manipulators", PhD Thesis, Carnegie Mellon University, Pittsburg.

Bergerman, M., Siqueira, A.G., Terra, M.H., 1999, "Underactuated manipulator control system development environment," *Proceedings of the 15th International Conference on CAD/CAM Robotics & Factories of the Future CARS&FOF99*.

Bergerman, M., Xu, Y., 1994, "Robust control of underactuated manipulators: analysis and implementation", *Proceedings of the 1994 IEEE International Conference on Systems, Man and Cybernetics*, pp. 925-930.

Chiang, R.Y., Safonov, M.G., 1992, "Robust Control Toolbox", The MathWorks.

Craig, J.J., 1986, "Introduction to Robotics – Mechanics and Control", Addison-Wesley.

Doyle, J.C., Francis, B.A., Tannembaum, A.R., 1992, "Feedback control theory", Maxwell Macmillan.

Doyle, J.C., Glover, K., Khargonekar, P.P., Francis, B.A., 1989, "State space solutions to standard H_2 and H_∞ problems," *IEEE Transactions on Automatic Control*, Vol. 34, pp. 831-847.

Kang, B.S., Kim, S.H., Kwak, Y.K., Smith, C.C., 1999, "Robust tracking control of a direct drive robot," *Journal of Dynamic Systems, Measurement, and Control*, Vol. 121, pp. 261-269.

Lewis, F.L., Abdallah, C.T., Dawson, D.M., 1993, "Control of Robot Manipulators", Macmillan Publishing Company.

Logan, C.L., 1994, "A comparison between H-infinity/mu-synthesis control and sliding-mode control for robust control of a small autonomous underwater vehicle", *Proceedings of the Symposium on Autonomous Underwater Vehicle Technology*, AUV '94, pp. 399-416.

Maciejowsky, J.M., 1989, "Multivariable Feedback Design", Addison-Wesley.

Safonov, M.G., Limebeer, D.J.N., Chiang, R.Y., 1989, "Simplifying the H_∞ theory via loop shifting, matrix pencil and descriptor concepts", *International Journal of Control*, Vol. 50, pp. 2467-2488.

Sage, H.G., de Mathelin, M.F., Ostertag, E., 1999, "Robust control of robot manipulators: a survey", *International Journal of Control*, Vol. 72, pp. 1498-1522.

Terra, M.H., Siqueira, A.A.G., Ishihara, J.Y., Barbeiro, T.L.S., 2003, "Control of underactuated manipulators via H_2, H_∞, H_2/H_∞ and mu-Synthesis", *Proceedings of the 4th IFAC Symposium on Robust Control Design – ROCOND03*, june 25-27, Milan, Italy.

Yao, B., Tomizuka, M., 1994, "Comparative experiments of robust and adaptive control with new robust adaptive controlleres for robot manipulators", *Proceedings of the 33rd Conference on Decision and Control*, pp. 1290-1295.

Youla, D.C., Saito, M., 1967, "Interpolation with positive-real functions", *Journal of The Franklin Institute*, Vol. 284, pp. 77-108.

Zhou, K., Doyle, J.C., Glover, K., 1995, "Robust and Optimal Control", Prentice Hall, 1995.

Zhou, K., Doyle, J.C., 1998, "Essentials of Robust Control", Prentice Hall.

Zhou, K., Glover, K., Bodenheimer, B., Doyle, J., 1994, "Mixed H_2 and H_1 performance objectives I: robust performance analysis", *IEEE Transactions on Automatic Control*, Vol. 39, pp. 1564-1574.

Zhou, K., Glover, K., Bodenheimer, B., Doyle, J., 1994a, "Mixed H_2 and H_∞ performance objectives II: optimal control", *IEEE Transactions on Automatic Control*, Vol. 39, pp. 1575-1586.